Materials Today: Proceedings xxx (xxxx) 1–6

Contents lists available at ScienceDirect

Materials Today: Proceedings

journal homepage: www.elsevier.com

Joint dissimilar diffusion bonding of SSM-ADC12 Al alloy to SSM 6063 Al alloy☆

C. Meengam [a, *], Y. Dunyakul [b], D. Maunkhaw [b]

[a] Faculty of Industrial Technology, Songkhla Rajabhat University, Songkhla 90000 Thailand
[b] Department of Industrial Engineering, Faculty of Engineering, Rajamangala University of Technology Srivijaya, Songkhla, Thailand

ARTICLE INFO

Keywords:
Diffusion Bonding
SSM-ADC12 Al Alloy
SSM 6063 Al Alloy
Dissimilar Joint

ABSTRACT

This experiment studied essential parameters for dissimilar diffusion bonding of SSM- ADC12 Al Alloy to SSM 6063 Al Alloy and the mechanism of diffused elements. This experiment indicated that 776 K for bonding temperature and 150 min for bonding time were suitable for welding this material because the bond line is complete. No physical deformation and no defects from welding were identified. The concentration of Si elements matrix composition diffused from 11.88 %wt to 8 %wt on SSM-ADC12 Al Alloy to SSM 6063 Al Alloy with a diffusion distance of 7.577 mm. The hardness was significantly increased by heat, stress compressive, and Mg_2Si intermetallic precipitation in the solid solution for 110.72 HV from SSM-ADC12 Al Alloy and 76.10 HV from SSM 6063 Al Alloy.

1. Introduction

Diffusion bonding or diffusion welding is one of the processes for solid-state welding. The diffusion bonding method is currently widely used in joining aerospace parts such as fuel tanks, heat exchangers, fuel injectors, gas turbines, and others [1]. Diffusion bonding was a joining technique suitable for alloys that are difficult to weld for dissimilar materials [2,3]. Typically, for the principle of diffusion bonding, the bonding temperature is approximately 50–80% of the melting temperature of particular materials [4,5] because it is the optimum temperature for atomic elements to diffuse at the joining interface. Therefore, the atoms moving between the interface result in the gap of the joint being eliminated and, at the right time, the samples could adhere to each other completely [6]. The diffusion bonding atmosphere is another factor that influences the adhesion of the samples.

Studies have shown that vacuum [7,8] and inert gas atmosphere such as argon gas [9,10] provide a positive effect on diffusion bonding because these could prevent the formation of oxide layers during the welding process [11,12]. Dissimilar joining diffusion bonding was used to solve the problems of bonded materials that cannot be melted together. However, the proper factor for dissimilar joining diffusion bonding is crucial because of the differences in the chemical composition of the welding material.

The SSM-ADC12 and SSM 6063 are Al Alloy developed to modernise the casting method and are widely used in the automotive and aerospace industry [13,14]. The casting in the semi-solid state affects the flows of the liquid metal and defects, defining a better mechanical property and microstructure. So, in this study, joint diffusion bonding between SSM-ADC12 Al Alloy and SSM 6063 Al Alloy was investigated in a butt-dissimilar rod welding format. This experiment aimed to study the diffusion mechanism at element levels in order to explain how the microstructural changes in the bonded line before and after welding. The investigators also looked for the relationship between welding parameters – bonding time, bonding temperature, bonding pressure, and atmospheric gas – and metallurgical properties of the finished samples. Moreover, the samples were tested for Vicker hardness to analyse the hardness changes resulting from heat during welding. After that, the appropriate parameters resulting from the study would be evaluated and proposed for a better and perfect welding protocol.

2. Experimental procedures

2.1. Materials

The materials in this experiment were produced by a Gas Induced Semi-Solid (GISS) process (As cast) [15]. The SSM-ADC12 Al Alloy was plated with cylindrical dimensions of Ø10 × 50 mm. Likewise, the SSM 6063 Al Alloy had the exact dimensions as the shape of the SSM-ADC12 aluminium alloy. The SSM 6063 and SSM-ADC12 Al Alloy had the formation of Mg_2Si intermetallics, which are plate-like shapes for Mg_2Si intermetallics and globular shapes for alpha (α) phase formation (Fig. 1). The materials used for the experiment were kindly provided as a complementary by GISSCO Company Limited, Songkhla, Thailand.

* Corresponding author.
E-mail address: Chaiyoot.me@skru.ac.th (C. Meengam).

https://doi.org/10.1016/j.matpr.2023.05.392
2214-7853/© 20XX

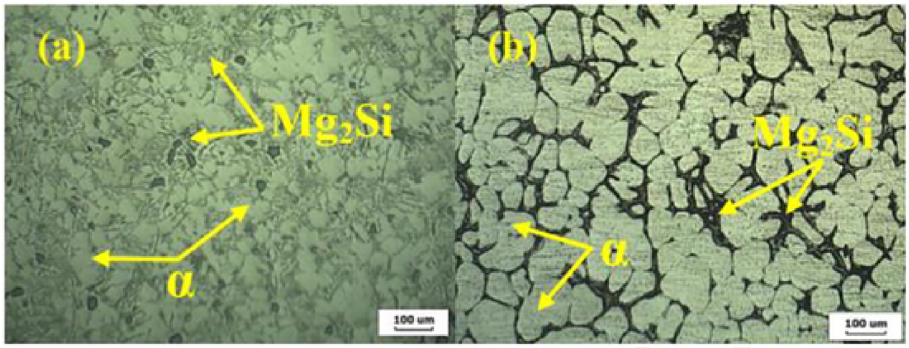

Fig. 1. Microstructure of base materials follow by (a) SSM-ADC12 and (b) SSM 6063 Al Alloy.

The chemical compositions of the two materials used in this experiment are shown in Table 1.

2.2. Experimental procedure

The surface preparation was polished with sandpapers with P1200 grit. The diffusion bonding process began with clamping the samples on a horizontal axis, with SSM-ADC12 Al Alloy on the left side, and on the contrary, with SSM 6063 Al Alloy on the right side. The guide bush and guide post supported the samples on a straight horizontal axis. Then, bonding pressure was constantly applied along the horizontal axis. When the sample fixing process was complete, the argon gas was released into the chamber to prevent oxides on the Al Alloy surface during diffusion bonding. And the bonding temperature was controlled according to the experimental conditions. The bonding temperature was considered in the range of 60%, 70%, and 80% of the melting point of SSM 6063 Al Alloy. The melting point for SSM-ADC12 Al Alloy was 582 °C, [16] while SSM 6063 Al Alloy had the melting point at 629 °C, [17]. The bonding temperature in the experiment was still in the solid state. The bonding time could be obtained from the preliminary experiment, which was noticed from the deformation of the samples. The diffusion bonding conditions in the study are shown in Table 2. However, during welding, in order to protect the samples diffused to the clamps; therefore, a ceramic cup was used to prevent the samples diffused to the clamps. The diffusion bonding process is shown in Fig. 2.

2.3. Mechanical and metallurgy analysis

The sample was prepared using the Vickers hardness test to evaluate the hardness properties of the bonded line. The Vicker's hardness tester was conducted on the Matsuzawa model MMT-X from Japan at a compression load of 10 gf on the diamond indenter for 10 sec, respectively. The metallurgy analysis was observed using a scanning electron microscope on FEI-Quanta model 400FEG from Switzerland to analyse elements' diffusion and distribution. Moreover, the defect and grain transformation were observed using the Optika microscope model: B-382PHi-ALC from Italy. Before metallurgy analysis, the surface of the samples was prepared by sandpaper polishing with P320, P600, P800, P1000, and P1200 grit, then was polished with alumina powder ranging 3–5 μm, and finally, etched with Keller's solution, respectively.

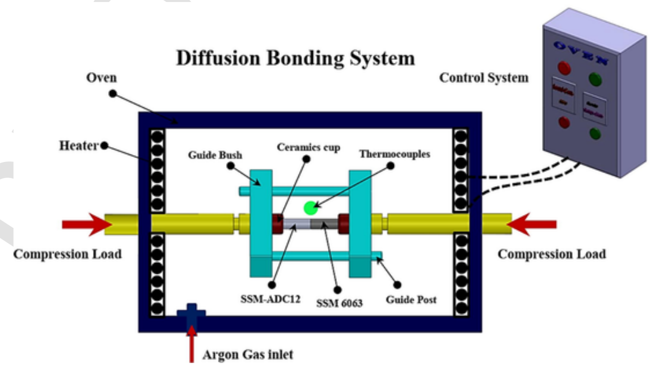

Fig. 2. Schematic diagram of SSM-ADC12 Al Alloy to SSM 6063 Al Alloy by diffusion bonding assembly.

Table 1
The compositions by wt% of SSM-Al Alloy were used in this study [13,14].

SSM-Al Alloy	Al	Mg	Si	Fe	Cu	Zn	Mn	Ti	Sn	Others
ADC12	Bal.	0.07	11.88	0.93	1.75	0.78	0.12	0.11	0.01	0.05
6063	Bal.	0.90	0.60	0.35	0.10	0.10	0.10	0.10	–	0.15

Table 2
The details of the dissimilar diffusion bonding conditions in this study.

Diffusion bonding parameter	Information
Bonding temperature (K)	650, 713 and 776
Bonding time (min)	90 and 150
Bonding Pressure (MPa)	3.82
Argon atmosphere (litre per min)	6

3. Results and discussion

3.1. Diffusion analysis

For the mechanism of elemental distribution around the bond line, the thermodynamics that results in the diffusion of high Si concentration are related to diffusion coefficient, diffusion activation energy, and bonding temperature. These three factors are the most critical parameters that affect the atomic diffusion explained in equation (1). [18]

$$D = D_0 e^{-(Q/RT)} \tag{1}$$

Equation (1) shows the parameters, which consist of: D represents the diffusion coefficient (m^2/s); D0 represents the diffusion coefficient (m^2/s); Q represents the atomic diffusion activation energy (J/mol); and R represents the Boltzmann constant, with a value of 8.314 J/(mol·K); finally, T represents the temperature (K) [19]. When the value of D0 is $1.8x10^5$ mm^2/s, and the value of Q is $4.61x10^5$ J/mol corresponding to elements Si, respectively. The Si elements with high concentrations in SSM-ADC12 Al Alloy will cause diffusion of Si atoms to SSM 6063 aluminium alloy, leading to a decrease in atomic volume but a good effect on the formation of Mg_2Si intermetallics.

The Si elements precipitating from Mg_2Si intermetallics can be calculated from the Gibbs free energy. The results in Fig. 3 showed that the increase of bonding temperature is likely to result in the reduction of the Gibbs free energy of Mg_2Si intermetallics. The bonding temperature

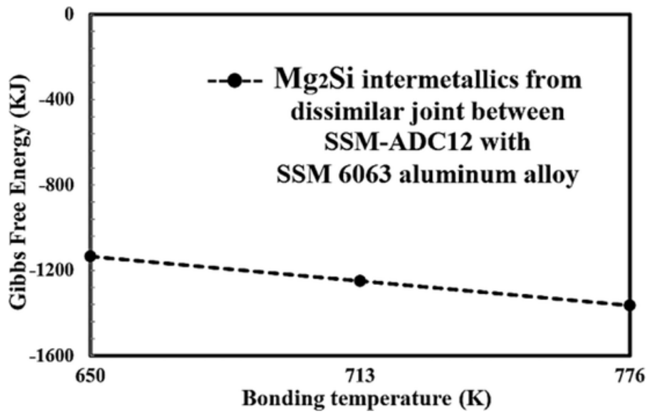

Fig. 3. Gibbs free energy of Mg_2Si intermetallics from diffusion bonding.

increase leads to the activation energy of the Si atom in SSM-ADC12 Al Alloy and brings about structural stability [20]. Besides, the lower Gibbs free energy results in atoms moving independently, leading to a greater atomic diffusion distance.

The distance of diffusion (X) is the relationship between diffusion coefficient (D), bonding time, and concentrations in the form of differential equations. Equation (2) describes the factors that affect the diffusion distance of atoms [21]. C represents the concentrations of Si elements (mol/mm^3), and the value is $7.74x10^{-3}$ mol/mm^3. t represents the bonding time, and D represents the diffusion coefficient (m^2/s).

$$X = C(Dt)^{1/2} \quad (2)$$

Equation (2) shows that diffusion coefficient and bonding time influence the distance of diffusion of atomic motion. According to Fig. 4, which shows Si atom diffusion distance, the longer the bonding time, the farther Si atoms move. It can be seen that the bonding time of

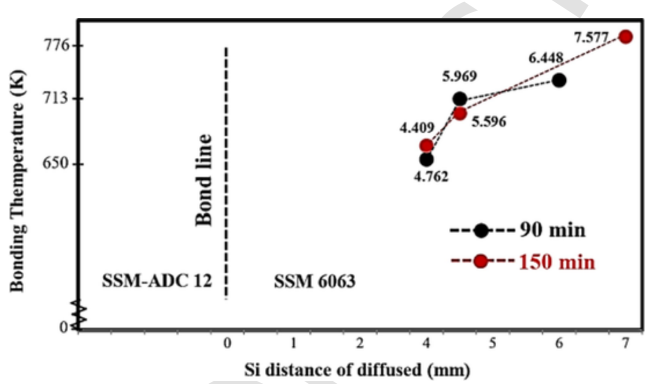

Fig. 4. Distance of atom diffusion on Si elements from SSM-ADC12 Al Alloy to SSM 6063 Al Alloy.

150 min tends to allow the Si atoms to diffuse at higher distances. At 650, 713, and 776 K, the diffuse distances are 5.969, 6.448, and 7.577 mm, respectively. On the contrary, with the bonding time of 90 min, Si atoms cannot move, with the diffuse distance of 4.409, 4.762, and 5.596 mm. The freedom of atomic motion is related to atomic size and vacancy. The smaller atomic size and larger vacancy there are, the longer distance the atoms can move [22]. The interstitial diffusion behavior happens in small atoms while the substitutional diffusion behaviour was observed in larger atomic sizes.

3.2. Metallurgy and defect analysis

The macro morphology of the diffusion welding samples is shown in Fig. 5. The quality of the physical characteristics of the samples is good, with no deflection, enlargement, and distortion. The heat diffuses into the centre of the suitable sample. As a result, the sample does not cause discontinuities of the joint. This causes the occurrence of fewer defects. However, the heat often affects the size of the grain. The cumulative heat can enlarge the interconnected grain boundary, leading to the grain size growing [23]. This growing grain usually expands further beyond the sample's centre (Fig. 5 (a-c)). Moreover, the heat also causes the elements to precipitate in the solid solution and causes plastic deformation. Therefore, bonding temperature and bonding time are essential parameters for diffusion welding. This experiment proved that the bonding temperature at 776 K and bonding time at 150 min were suitable because of the best adhesion ability of the samples, with no defect indicator and no deformation after welding. For the longer bonding time and temperature above 80 percent of the melting point of the material, deformation on the samples after welding was observed [24]. Vice versa, shorter bonding time and the temperature usually cause non-successful diffusion welding bonding time at 150 min.

Fig. 6 shows SEM images with the top surface of the bond line. The increase of bonding time and bonding temperature significantly reduces the defect. As a general observation of the bonding time above 150 min with the range of bonding temperature from 650 to 776 K, the bond sound tended to increase when the bonding time was increased. On the contrary, the lower bonding time at 90 min tended to form a poor sample adhesion ability because of the too little mobility time of the atoms of the two materials to be exchanged. As a result, the voids between the two material contact surfaces are not eliminated. Another factor that affects the good adhesion of diffusion bonding is the different chemical composition concentrations of the two samples. The higher the different chemical composition concentrations are, the more atoms allow to easily diffuse to each other [25]. So, if more atoms can be completely diffused into the other sample, this diffusion bonding process is successfully bonded. The only type of defect discovered in this study was voids with characteristics that are parallel to the direction of the joint. The voids will undergo shrinkage and have a size and volume smaller until, eventually, those voids are eliminated, leading to the two materials being homogeneous together. However, diffusion bonding in the air and gas atmosphere often found oxygen infiltra-

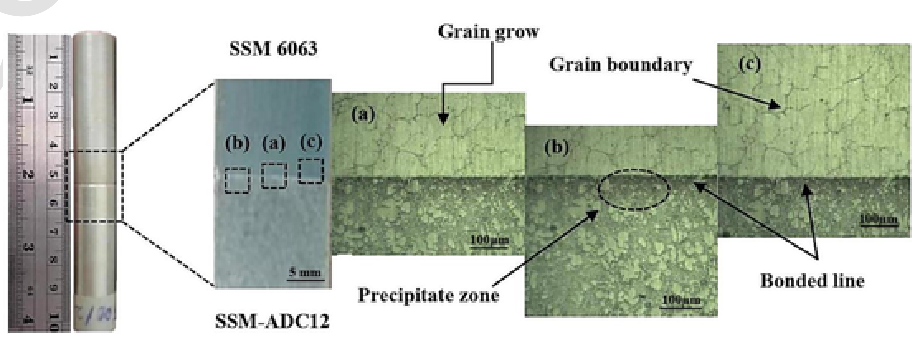

Fig. 5. Macro morphology of dissimilar of SSM-ADC12 Al Alloy with SSM 6063 Al Alloy from bonding temperature at 776 K and.

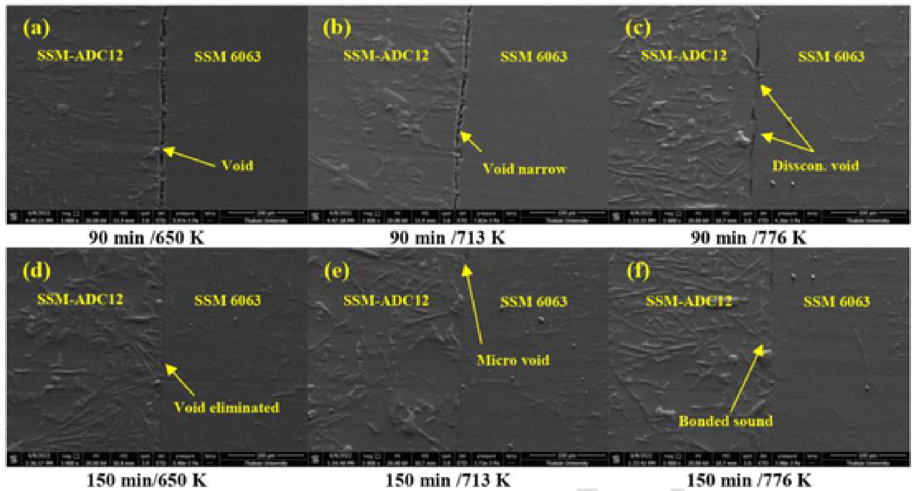

Fig. 6. Influence of bonding time and bonding temperature on microstructural transformation effect.

tion within the void area, where oxygen is a barrier to the diffusion of elements [26]. Regarding microstructural changes, Mg_2Si intermetallics from SSM-ADC12 Al Alloy diffused to SSM 6063 aluminium alloy. Whilst, Mg_2Si intermetallics from SSM 6063 Al Alloy have a low diffusion ability because of the low concentration of elements. Normally, the structural changes and the formation of defects often adversely affect the mechanical properties of the sample after welding.

The EDX can be evaluated regarding microstructural changes shown in Fig. 7, which is found that the bond line of the two materials in the experiment was well homogeneous (Fig. 7(a))., and the Mg_2Si intermetallics precipitated in the solid solution (Fig. 7(b)). The atoms of Si elements can be moved further due to high concentration (Fig. 7(d)). The Si elements at 11.88 %wt from SSM-ADC12 Al Alloy can easily diffuse to SSM 6063 Al Alloy. On the other hand, Si elements SSM 6063 Al Alloy have increased significantly. Meanwhile, Al as the primary metal is still prevalent in the bond line (Fig. 7(c)). Mg elements showed good dispersibility at high temperatures and distributed evenly throughout the bond line in a non-clustered manner shown in Fig. 7(e). However, it is observed that O elements which are residues from the gas atmosphere. Diffusion welding influences the combination of other elements to form SiO_2, MgO, and Al_2O_3 intermetallics (Fig. 7(f and h)). The O elements condensed to form oxides which are problems for atomic motion in experimental materials [27] because the oxide has a high melting temperature and causes a thin film formation, preventing the diffusion of atoms during diffusion welding. Another problem with oxides at the joints of the samples is that these oxides could obstruct the voids eliminating mechanism [28], resulting in unsuccessful welding. The diffusion welding is therefore recommended to be welded under vacuum conditions. Therefore it will provide better performance than other states. This experiment also found some C elements around the bond line (Fig. 7(g)) and hypothesized that this came from the stainless steel used to manufacture the fixture.

3.3. Vickers hardness analysis

The hardness is shown in Fig. 8. In this experiment, the results were consistent and in the same direction in all trials. Therefore, we would like to explain that the most optimal parameters are bonding temperature at 776 K and bonding time of 150 min. It is also found that, in every area of the samples, the hardness is increased because of the heat during welding resulting in the precipitation of Mg_2Si intermetallics, similar to the samples' heat treatment [29]. The hardness from SSM-ADC12 Al Alloy was significantly increased to 110.72 compared to the base hardness value at 97.12 HV while the hardness of SSM 6063 Al Alloy was increased to 76.10 HV compared with the base hardness value

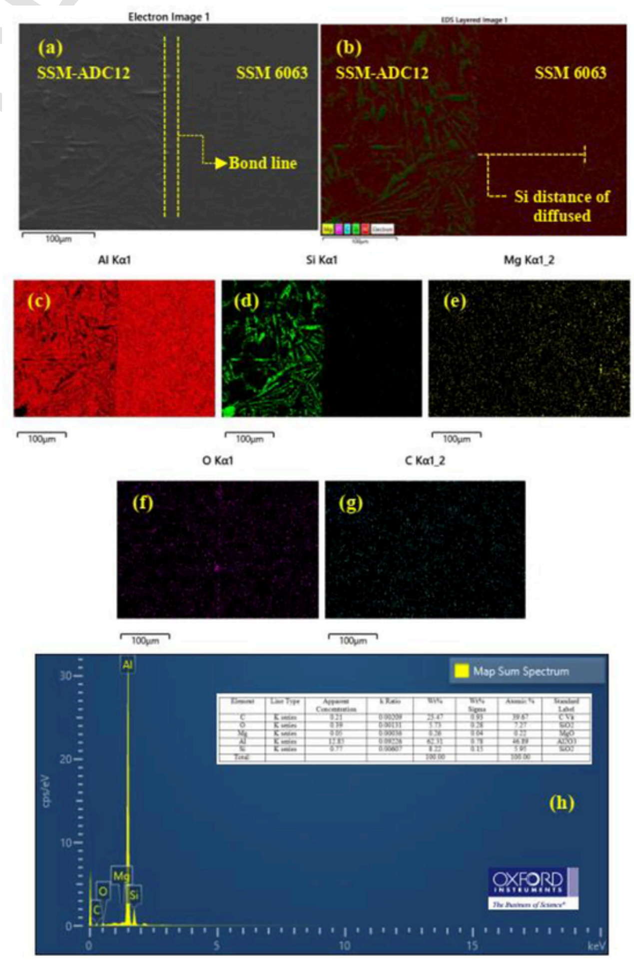

Fig. 7. Microstructural evaluation in bond line from dissimilar materials by diffusion welding: (a) SEM micrographs, (b) Mapping micrographs and (c-h) EDX micrographs.

at 67.31 HV. The stress concentration in the bond line from compressive is another factor to increase in hardness around the bond line [30]. However, the hardness properties may decrease for an extremely long bonding time because it affects the growth of grain, leading to ductility.

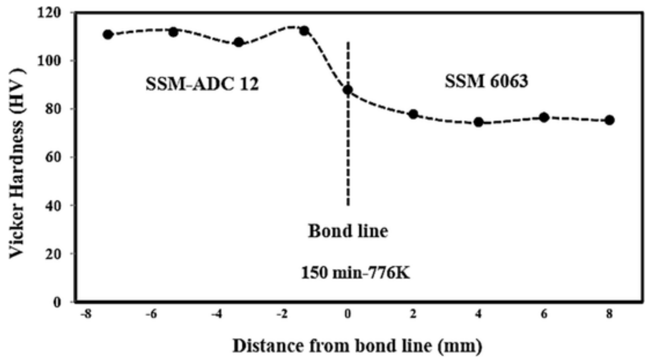

Fig. 8. The microhardness profile across the SSM-ADC12 with SSM 6063 Al Alloy bond line after diffusion bonding.

4. Conclusion

In this experiment, the evaluation of essential parameters of dissimilar diffusion welding between the SSM-ADC12 and SSM 6063 Al Alloy could be concluded in the following:

(1) The suitable parameters in experiments were bonding temperature at 776 K and bonding time at 150 min resulting in no deflection, enlargement, and distortion after welding.

(2) The higher the bonding temperature influence Gibbs free energy of Mg_2Si intermetallics to decrease, leading to good movement of atoms. At 776 K for bonding temperature and 150 min from bonding time, particles of Si elements can be diffused further 7.577 mm away from the bond line.

(3) The EDX examination found that the high concentration of the Si elements was changed from 11.88 %wt on SSM-ADC12 Al Alloy to only 8% concentration left by diffusing to SSM 6063 Al Alloy.

(4) After diffusion bonding, it showed a significant hardness increase due to the heat causing the precipitation in the solid solution of Mg_2Si intermetallics during welding.

(5) the optimal conditions to weld these SSM-ADC12 Al Alloy to SSM 6063 Al Alloy together is bonding temperature at 776 K, bonding time at 150 min, and bonding Pressure at 3.82 MPa with Argon atmosphere for 6 L per min.

CRediT authorship contribution statement

C. Meengam : Conceptualization, Data curation, Funding acquisition, Investigation, Methodology, Project administration, Software, Writing – original draft, Writing – review & editing. **Y. Dunyakul :** Formal analysis, Investigation. **D. Maunkhaw :** Data curation, Supervision, Validation, Visualization.

Declaration of Competing Interest

The authors declare that they have no known competing financial interests or personal relationships that could have appeared to influence the work reported in this paper.

Data availability

No data was used for the research described in the article.

Acknowledgements

The materials for this work were supported by the GISSCO Company Limited and by research grants from the Faculty of Industrial Technology, Songkhla Rajabhat University, and the Faculty of Engineering, the Rajamangala University of Technology Srivijaya from Thailand.

References

[1] H.-S. Lee, Diffusion bonding of metal alloys in aerospace and other applications, Woodhead Publishing, 2012, pp. 305–327.
[2] Y. Li, P. Liu, J. Wang, H. Ma, XRD and SEM analysis near the diffusion bonding interface of Mg/Al dissimilar materials, Vacuum 82 (1) (2007) 15–19.
[3] W. Jie, F. Yang, Z. Fuqi, X. Qinglian, X. Yanlin, Y. Haotian, X. Qinghai, Microstructure and mechanical property of SiC whisker coating modified C/C composite/Ti_2AlNb alloy dissimilar joints prepared by transient liquid phase diffusion bonding, Ceram. Int. 46 (5) (2012) 5937–5945.
[4] N.F. Kazakov, Procedures for diffusion bonding in vacuum, Amazon Publishing 82 (1) (1984) 47–70.
[5] R. Dipin Kumar, Y. Koli, S. Aravindan, Interface-free novel joining of additively manufactured Al-Si 5wt.% alloy through diffusion bonding, Mater. Lett. 337 (2023) 133976.
[6] R.J. Mu, Z.W. Yang, S.Y. Niu, K.B. Sun, Y. Wang, D.P. Wang, Diffusion bonding of $(Hf_{0.2}Zr_{0.2}Ti_{0.2}Ta_{0.2}Nb_{0.2})C$ high-entropy ceramic with metallic Ni foil, J. Eur. Ceram. Soc. 41 (15) (2021) 7478–7487.
[7] P. Li, C. Li, H. Dong, W.u. Baosheng, Y. Ma, C. Zou, Y. Yang, Vacuum diffusion bonding of TC4 titanium alloy to 316L stainless steel with $AlCoCrCuNi_2$ high-entropy alloy interlayer, J. Alloys Compd. 909 (2021) 164698.
[8] W.u. Baosheng, H. Dong, P. Li, Y. Ma, Y. Yang, C. Zou, C. Li, Vacuum diffusion bonding of TC4 titanium alloy and T2 copper by a slow cooling heat treatment, J. Mater. Process. Technol. 305 (2022) 117595.
[9] S.S.K. Ardestani, V. Dashtizad, A. Kaflou, Experimental investigations on time, temperature and atmosphere influence on microstructure and mechanical properties of borosilicate glass to Kovar-alloy seals, Mater. Charact. 171 (2021) 110805.
[10] Y. Zhu, Y.u. Mingyang, Q. Lv, H. Hou, J. Yang, G. Liu, J. Liu, G. Qiao, Effects of the high-temperature sensitization in argon atmosphere on the microstructure and properties of polycrystalline PbSe films, Mater. Sci. Semicond. Process. 162 (2023) 107486.
[11] Z. Wang, C. Li, X. Si, Y. Liu, J. Qi, Y. Huang, J. Feng, J. Cao, Oxidation behavior of ferritic stainless steel interconnect coated by a simple diffusion bonded cobalt protective layer for solid oxide fuel cells, Corros. Sci. 172 (2020) 108739.
[12] P.u. Zhao, Z. Li, X.u. Zhiwu, X. Leng, A. Tong, J. Yan, Migrating behaviors of interfacial elements and oxide layers during diffusion bonding of 6063Al alloys using Zn interlayer in air, JMST 155 (2023) 119–131.
[13] C. Meengam, K. Sillapasa, Evaluation of optimization parameters of semi-solid metal 6063 aluminum alloy from friction stir welding process using factorial design analysis, J. Manuf. Mater. Process. 4 (123) (2020) 1–20.
[14] S. Chainarong, T. Srichok, R. Pitakaso, W. Sirirak, S. Khonjun, R. Akararungruangkul, Variable neighborhood strategy adaptive search for optimal parameters of SSM-ADC 12 aluminum friction stir welding, Processes 9 (1805) (2021) 1–24.
[15] T. Chucheep, R. Burapa, S. Janudom, S. Wisutmethangoon, J. Wannasin, Semi-solid gravity sand casting using gas induced semi-solid process, Trans. Nonferrous Met. Soc. 20 (3) (2010) s981–s987.
[16] Suppachai Chainarong, Rapeepan Pitakaso, Worapot Sirirak, Thanatkij Srichok, Surajet Khonjun, Kanchana Sethanan, Thai Sangthean. Multi-Objective Variable Neighborhood Strategy Adaptive Search for Tuning Optimal Parameters of SSM-ADC12 Aluminum Friction Stir Welding. J. Manuf. Mater. Process. 5(4):123, (2021) s981-s987
[17] C. Meengam, K. Sillapasa, Y. Pratumwal, S. Otarawanna, Effects of Heat dissipation from friction stir welding to microstructures of semi-solid cast 6063 Al alloy, Key Eng. Mater. 904 (2021) 70–75.
[18] Y. Li, D. Yang, W.u. Zhisheng, W. Yang, C. Liu, Effect of Annealing temperature on microstructure and properties of Al/Mg magnetic pulse welding joints, Materials 15 (5519) (2022) 1–14.
[19] M. Moslemi, K. Javaherdeh, H.R. Ashorynejad, Effect of compression of microporous and gas diffusion layers on liquid water transport of PEMFC with interdigitated flow field by Lattice Boltzmann method, Colloids Surf. A 642 (2022) 128623.
[20] C. Meengam, Y. Dunyakul, D. Mueankhao, S. chainarong, Transient liquid phase bonding of semi-solid metal 7075 aluminum alloy using ZA27 zinc alloy interlayer, Metals 8 (637) (2018) 8080637.
[21] L. Li, L. Sun, M. Li, Diffusion bonding of dissimilar titanium alloys via surface nanocrystallization treatment, J. Mater. Res. Technol. 17 (2011) 1274–1288.
[22] L. Gao, H. Zhang, Z. Zhang, Ingeniously introducing of boron to adjust hetero-atoms and their bonding with cobalt for improving the catalysis of oxygen reduction reaction, J. Solid State Chem. 289 (2020) 121523.
[23] Y.u. Peng, J. Li, Z. Li, S. Li, W. Guo, X. Gao, J. Xiong, Interfacial voids and microstructure evolution, bonding behavior and deformation mechanism of TC4 diffusion bonded joints, J. Manuf. Process. 81 (2022) 837–851.
[24] P. Lin, X.I. Xian-zheng, Z.H.A.O. Wen-kai, Y.A.N.G. Rui-hong, L.I.N. Fei, C.U.I. Xiao-lei, L.I.U. Gang, Microstructure and mechanical properties of Ti-6Al-4V/Ti-22Al-25Nb joint formed by diffusion bonding, Trans. Nonferrous Met. Soc. 31 (5) (2021) s981–s987.
[25] K. Liu, X. Cui, M. Dong, Z. Xing, J. Li, H. Tian, G. Jin, H. Wang, X.u. Binshi, Mechanism of diffusion promotion of carbon atoms during carburization of 20Cr2Ni4A alloy steel after lanthana-bearing supersonic fine particle bombarding pretreatment, Surf. Coat. Technol. 425 (2021) 127702.
[26] Yuanyuan Chen, Yuan Huang, Fei Li, Lu Han , Dongguang Liu, Laima Luo, Zongqing Ma, Yongchang Liu, Zumin Wang. High-strength diffusion bonding of oxide-dispersion-strengthened tungsten and CuCrZr alloy through surface nano-

activation and Cu plating Technol. J. Mater. Sci. Technol. 92 (2021) 186-194.
[27] H.-S. Lee, J.-H. Yoon, Y.-M. Yi, Oxidation behavior of titanium alloy under diffusion bonding, Thermochim. Acta Mater. 445 (1–2) (2007) 105–108.
[28] N. Esakkiraja, A. Gupta, V. Jayaram, T. Hickel, S.V. Divinski, A. Paul, Diffusion, defects and understanding the growth of a multicomponent interdiffusion zone between Pt-modified B2 NiAl bond coat and single crystal superalloy, Acta Mater. 195 (2020) 35–49.
[29] Yi Xiao, Lihui Lang, Wencai Xu, DexinZhang. Diffusion bonding of copper alloy and nickel-based superalloy via hot isostatic pressing. J. Mater. Res. Technol. 19 (2022) 1789-1797.
[30] F. Wang, L. Han, J. Zhong, Stress-induced atom diffusion at thermosonic flip chip bonding interface, Sens. Actuator A Phys. 149 (1) (2009) 100–105.